Biointerface Research in Applied Chemistry
Open-Access Journal (ISSN: 2069-5837)

Article
Volume 13, Issue 6, 2023, 512
https://doi.org/10.33263/BRIAC136.512

Erosive Wear Behavior of Carbon Black/Bio-char Bio-waste (Orange Peel) Reinforced Composites

Prajapati Naik [1,2], Smitirupa Pradhan [3], Prasanta Sahoo [1,*], Samir Kumar Acharya [4]

[1] Department of Mechanical Engineering, Jadavpur University, Kolkata, India
[2] Department of Mechanical Engineering, National Institute of Science and Technology, Berhampur, India
[3] School of Mechanical Engineering, KIIT Bhubaneswar, India
[4] Department of Mechanical Engineering, National Institute of Technology, Rourkela, India
* Correspondence: psjume@gmail.com; prasanta.sahoo@jadavpuruniversity.in (P.S.);

Scopus Author ID 55562055400
Received: 22.10.2022; Accepted: 24.11.2022; Published: 2.01.2023

Abstract: In the present work, carbon black (CB) /bio-char is utilized as a reinforcing material to fabricate a new set of polymer composites where thermoplastic epoxy resin acts as a matrix material. The CB material was synthesized from orange peel particulate (a bio-waste material) by pyrolysis at a carbonization temperature of 800°C. The erosive wear (EW) of fabricated specimens was examined at various operating conditions, such as selecting four impact angles (30°, 45°, 60°, and 90°), selecting three impact velocities (48, 70, and 82 m/s) and angular abrasive particles (silica sand of range 200±50µm) as per ASTM G76 standard. The experimental investigation reveals that the EW behavior of CB-reinforced composite decreases with increasing the filler loadings. The minimum wear rate is observed in 20 wt % CB filler loadings. Irrespective of the filler loadings, the maximum erosion occurs at 45° and 60° impact angles for low (48 m/s) and high impact velocities(82 m/s), respectively. All the fabricated composites exhibit semi-ductile behavior towards EW analysis. When the erodent velocity increases, the material removal rate (MRR) increases. The reported data were extracted from experimental results under controlled laboratory conditions. The eroded surfaces were analyzed by scanning electron microscopy to study the morphological characteristics for validating the experimental results. Other possible approaches, such as XRD analysis and energy dispersive x-ray analysis, have also been discussed in this article.

Keywords: bio-waste;bio-char; composite; SEM;erosive wear; energy dispersive spectroscopy.

1. Introduction

Nowadays, environmental pollution and global warming are worldwide catastrophes, which have forced several researchers and the scientific community to think about using natural materials to produce green products and diminish the emission of harmful carbon dioxide (CO_2). Currently, several researchers meticulously investigate the possible use of natural fibers/bio-waste fibers to cut down CO_2 emissions and conserved non-renewable resources instead of synthetic fibers in the composite industries. A number of researchers studied the bio-fibers such as jute, coir, sisal, and banana [1-4] and found them suitable as reinforcement in polymer industries. Due to some handy properties of bio-waste materials, such as low-cost, lightweight, nontoxicity, biodegradability and easy availability, and high specific modulus, etc., have encouraged the research community to observe their probability as reinforcement in polymer (composite) industries [5-8]. Due to the above-mentioned properties, the bio-waste

materials might be used as reinforcement instead of synthetic fiber in producing low-cost materials used in household components like doors and windows, etc. Natural fibers have a crucial role in advancing high-performance, eco-friendly composites [9]. Out of the different modes of failure of materials, erosion wear is one among them, which generally damages different components starting from structural components like helicopter rotor blades and gas turbine blades to household components like doors and windows, etc. [10-12]. Hence, it is considered a serious problem and has been studied by many researchers for different composite specimens, from metal to polymer matrix composites. Pradhan and Acharya researched the erosion rate of *Eulaliopsis binata* polymer composite. They observed that the erosive behavior of *Eulaliopsis binata* fiber-reinforced specimen changes from a brittle to semi-ductile nature. They also reported that maximum erosive resistance is observed in the case of 30 wt% fiber loadings [8]. Gupta *et al*. investigated the tribological behavior of cenosphere fly ash-reinforced bamboo fiber composites [13]. They observed that the wear rate of the specimen is extensively exaggerated by the size of the erodent, impact velocity, impact angle, and filler loading. They also reported a major improvement of the erosive wear resistance of fabricated specimens by adding cenosphere fly ash. Naik *et al*. investigated the erosive wear behavior of orange peel particulate (OPP) reinforced polymer composite materials. They reported a major improvement in inerosive wear resistance due to OPP filler loadings [14]. Nayak and Mohanty studied the erosive wear behavior of randomly oriented benzoyl chloride-treated areca sheath fiber-reinforced polyvinyl alcohol composites. They found maximum erosion at a 45° impact angle irrespective of fiber loadings. However, minimum erosion was recorded at 10 wt % fiber loadings [15]. The erosion behavior of glass fiber and silicon carbide-reinforced polymer composites has been studied by Antil *et al*. [16]. They observed that the size of reinforcement and impact angle are the dominating factors affecting the specimen surface's erosive resistance.

However, the applications of natural fibers reinforced composite material are restricted due to certain drawbacks such as weak interfacial adhesion, poor wettability, high rate of moisture absorption, and vulnerability to bacteria/fungal attacks [17]. Bio-fibers may be used in polymer industries to get low-cost value-added products after carbonization at different carbonization temperatures. The interfacial bonding between polymer composite components increases after bio-filler materials carbonization[18]. Nowadays, researchers give much more attention to developing low-cost materials such as bio-char, carbon black (CB), and activated CB from the lingo cellulosic bio-waste/agricultural waste material. The CB is manufactured from bio-waste material by various thermal decomposition processes such as gasification, liquefaction, combustion, and pyrolysis processes in anoxic conditions.

Minugu *et al*. investigated the erosion behavior of bio-char reinforced polymer composites. They extracted biochar from bael sells and arhar stalks and found that carbon is the main constituent in biochar. They found that polymer composite's erosion behavior decreases extensively compared to bael shell and arhar stalks bio-char reinforced composites [19]. Johnson *et al*. extracted biochar from sawdust by slow pyrolysis process at 700°-800°C. They observed that the erosive resistance increases by about 68% by adding 10 wt% bio-char to sansevieria cylindrical reinforced vinyl ester composite compared to unfilled bio-char composite [20]. M. Sutikno [21] worked in carbonized coconut char powder and suggested that the CB can replace graphite to fabricate automotive brake friction material. Ojha *et al*. [22] developed the CB material by using waste wood apple shells with the help of the pyrolysis process at different carbonization temperatures. They reported that the addition of CB filler enhances the mechanical properties significantly compared to neat polymer composite.

Samantarai *et al*. [23] researched the wear behavior of the bio-char reinforced polymer composite and found that the wear resistance increases with the addition of rice husk biochar. Betancourt *et al*. [24] investigated the wear behavior of novolac phenolic resin matrix composites prepared by slow pyrolysis. They observed an increase in wear resistance due to the addition of carbon fiber in composite material. Generally, solid CB materials, either amorphous or crystalline, have the lowest erosive wear (EW) behavior. Mauro Gioreclli *et al*. [25] noticed that the biochar epoxy composite changes its nature from brittle to ductile due to the presence of biochar. The biochar was synthesized from Maple tree blocks by pyrolysis in an inert atmosphere at 600°C and 1000°C. Based on the literature review, it is concluded that the EW rate is improved with CB filler loadings.

Several works have been done on the mechanical and physicochemical properties of biochar composites, available in several scientific articles. However, very few pieces of literature are available about the tribological behavior of bio-char reinforced composite materials. This research work mainly aims to convert bio-waste material into a value-added product. In this work, the erosive behavior of the developed specimen has been studied under various operating parameters such as impact angle, impact velocity, and filler loadings. Therefore, the CB material has been developed by the pyrolysis process at 800^{o}C carbonization temperature, and the characterization of CB filler has been done by EDS analysis and SEM analysis.

2. Materials and Methods

2.1.Carbon black particles through carbonization (Pyrolysis) process.

Cellulose, hemicelluloses, essential oils and proteins, and some simple carbohydrates are the main constituents of orange peels (OP), the outer cover part of the orange. The OP is to be used for the experimental purpose and was cleaned repeatedly with distilled water to remove impurities and unwanted particles. After that, the materials were sun-dried till the removal of moisture content. Then, the OP particulates were ground into small segments using a crusher. The small segments were ground into powder form using a planetary ball milling device. The surface of the material increases after using a planetary ball milling device [26]. A sieve shaker was used for sieve analysis. Sieve shakers with various mesh sizes were used to achieve different particle sizes, i.e., 1 µm to 212 µm. The entire procedure is explained in Figure 1.

The carbonization process is used to enhance the carbon content and microporosity structure in the natural fiber. The process was carried out in a specially designed burning furnace (Figure 2), through which a calculated amount of air is to be supplied. The OP particulates were kept in a ceramic boat inside a muffle furnace under an inert atmosphere. The temperature of the furnace increases to 800°C at a rate of 5°C/min. During the carbonization process, to maintain an inert environment, nitrogen gas was supplied to the chamber to avoid oxidation, which caused ash. After getting the required temperature, the specimens were soaked at the above-said temperature for one hour and then cooled in the furnace. Figure 3a shows the CB materials obtained from the furnace. Subsequently, the CB materials were ground and sieved, as shown in Figure 3b, for further analysis. The property of the CB material obtained from the natural fiber greatly depends upon the material's heating rate, carbonization temperature, and soaking time.

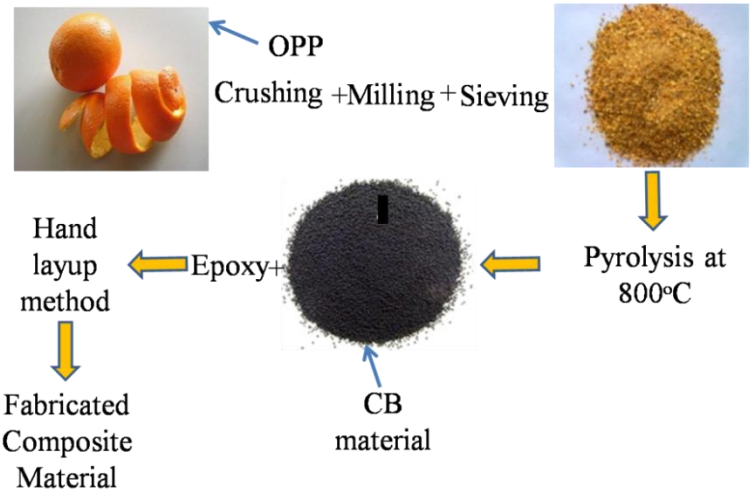

Figure 1. Procedure for fabrication of composite material.

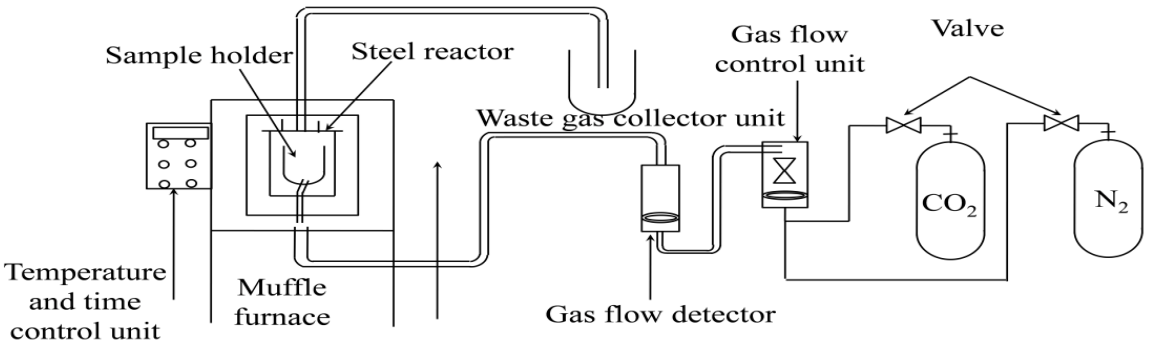

Figure 2. Special design burning chamber (furnace).

Figure3. Carbon black (CB) powder of OPP: **(a)** crystalline structure and **(b)** amorphous.

2.2.XRD analysis.

Usually, the XRD technique is applied to assess the crystallinity of the cellulose. It helps for qualitative and semi-qualitative assessment of cellulosic components in a material. It is also used to evaluate the strain, chemical proportion, and size of the material's crystalline structure. The typical characteristics of crystal structures are noticed in the form of peaks in this analysis. Sharp peaks and single broad diffused peaks represent the compounds' crystalline structure and amorphous structure, respectively.

2.3.SEM analysis.

The morphology of the CB surfaces and worn surface of the tested specimens has been observed by Nova Nano SEM450. The broken parts of the specimens were cut and fixed in a circular disc with tape. To make the surface conducting, the samples were coated with

platinum. The specimens were subjected to a high accelerating voltage range of 10 to 15 kV during the analysis. The micrographs of specimens were captured under different magnifications. The aim of the SEM analysis is to analyze the effect and consequence of wear behavior and also to validate the experimental results.

2.4.EDX (energy-dispersive X-ray) analysis.

EDX analysis is the method through which the elemental compositions of different materials can be determined. It is a surface analytical technique where an electron beam targets the sample. Due to the bombardment of the electron beam, there is the movement of electrons in the inner shell of the material. This causes the formation of an electron hole in the element's structure.

2.5 EW test setup and mechanism.

A solid particle erosion test rig has studied the erosive wear of different specimens (Figure 4a) as per ASTM G76–95 standards. Different components include the erodent feeder, erodent nozzle, conveyor belt system, air particle mixing and accelerating chamber, nozzle, specimen holder, angle adjustment knob, an air compressor, and erodent sand collector are shown in Figure 4b. The angular shape silica sand (erodent) abrasive particles of dimension 200±50 µm were supplied to the conveyor belt at a fixed rate and mixed with dry compressed air in the mixing chamber. The accelerated erodent particles hit the sample at high velocity. An adjustable sample holder was used to fix the targeted sample at different angles (such as 30°, 45°, 60°, and 90°) w. r. t the erodent particles. The erodent feed rate is 2±0.02 (gm/min). The experiments were conducted at different pressures, and with the help of a pressure regulator knob; pressure was adjusted as per requirement. The standoff distance (distance between the nozzle and the sample) is 10 mm. For each test, five different samples of the same dimensions were taken under the same operating conditions, and the operating parameters are given in Table 1.

Acetone is used to clean the sample and then weighed prior to the experiment by a pan electronic weight machine with a precision of 0.001 gm. The weighted sample is fixed in the erosion rig with the required impingement angle and subsequently eroded for 10 minutes. Weight loss of the eroded sample (W_m) is estimated by taking the difference between the initial and final weights. The erosive wear (E_r) is determined by using the equation

$$E_r = W_m / W_e ,$$

where W_m and W_e represent the weight loss of the composite material (gm) and weight of erodent particles (testing time ×particle feed rate). The erosion efficiency was calculated using the equation proposed by Sunderrajan *et al*. [27], whereE_r is the steady state erosion rate, H and ρ are the hardness and density of the target material, respectively and v is the velocity of an erodent particle.

From the literature, it is observed thatthe EW of polymer composite is mainly depending upon the impact angle and impact velocity. If maximum erosion was recorded at a low impact angle, i.e., between 15° to 30°, the material behaves ductile behavior, and for brittle material, maximum erosion occurs at a 90° impact angle [28]. However, if the maximum erosion was recorded between 30° to 45° and 60° to 90°, then the material exhibits semi ductile and semi-brittle nature, respectively. Pure epoxy composite is brittle in nature, as maximum erosion was recorded at a 90° impact angle [29, 30]. The EW behavior of polymer composite

with respect to impact velocity can be calculated by using the equation, $E_r = k \times v^n$, where E_r is the erosive wear rate. Power law has been used to estimate the k (velocity constant) and n (velocity exponent) values by fitting the data points on the EW rate with respect to impact velocity. The value of n was calculated from the EW equation used to study the nature of the material toward erosive wear. The material behaves as ductile when n lies between 1 and 2 and brittle when n lies between 4 and 6. However, if it lies between 2 and 3 and 3 and 4, the material shows semi-ductile and semi-brittle behavior towards EW.

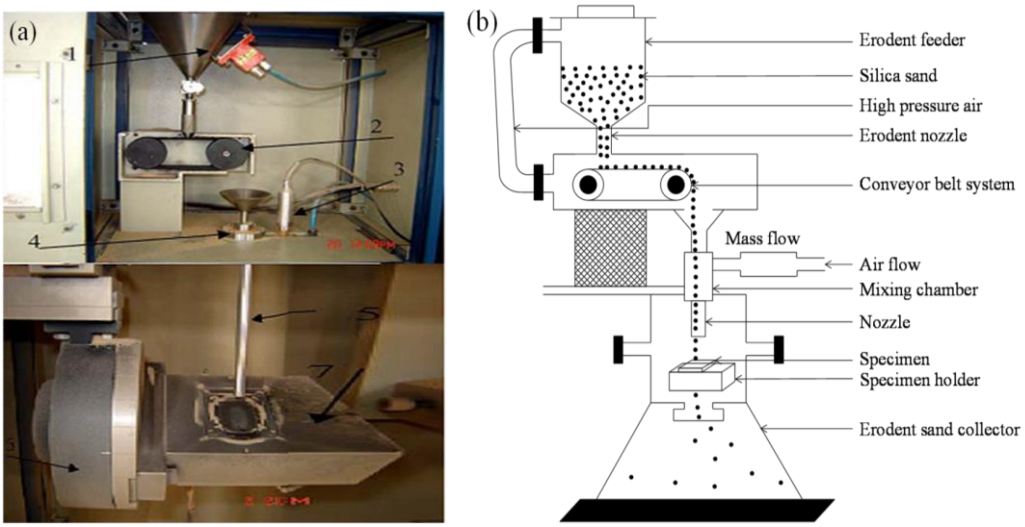

Figure 4. (a) EW test apparatus and **(b)** Schematic of jet erosion test rig.

Table 1. Erosive wear experiment operating parameters.

Components	**Parameters**	**Units**
Erodent	Silica sand	-
Avg size of Erodent size	150-250	µm
Erodent shape	Irregular, slightly rounded	
Impact angle (α)	30, 45, 60 and 90	°
Erodent velocity (v)	48, 70 and 82	m/s
Feed rate of erodent	2±0.02	gm/min
Experiment temperature	Ambient temperature	°C
Distance of sample from nozzle	10	mm
Nozzle diameter	4	mm

3. Results and Discussions

Different analyses have been done based on experimental results for polymer-based composite reinforced with OPP CB as follows:

3.1. SEM analysis of CB.

Figure 5 shows the microstructure of the CB filler. Several porous structures are observed on the surface of the filler. The development of porous structures on the surface of CB particles is due to a reduction of more amount of volatile matter at higher carbonization temperatures.

3.2. EDX analysis.

Due to carbonization, pyrolysis slowly removes non-carbon elements from the raw OP particulates, after removing non-carbon elements, the percentages of carbon increase along with the increment of some other elements which are presented in Figure 6. The percentage of different elements observed from EDX analysis is presented in Table 2.

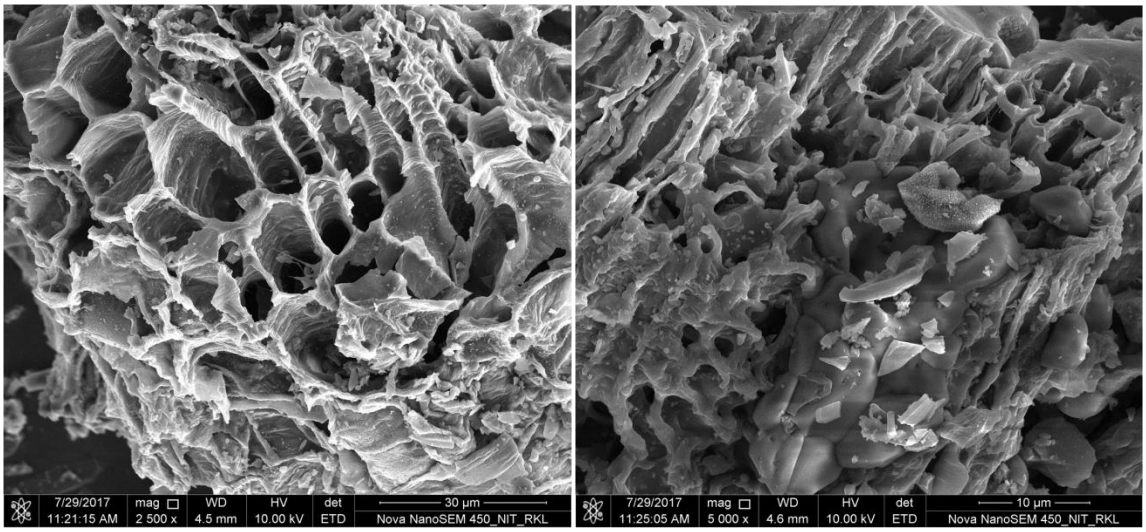

(a) (b)

Figure 5. Surface morphology of CB filler: (a) at 2500x (b) at 5000x

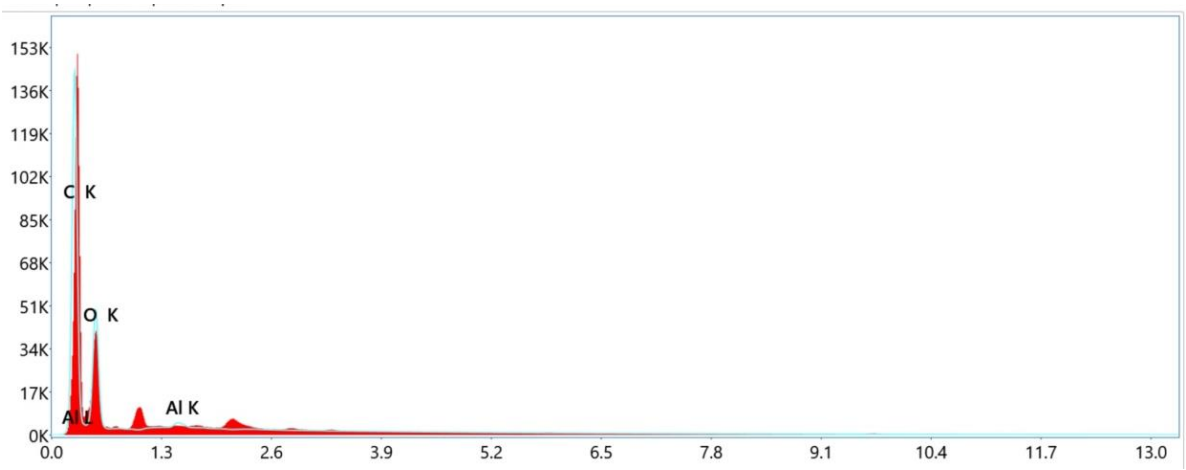

Figure 6. EDS analysis: 800ºC.

Table 2. Percentage of different components.

Element	Weight %	Atomic %	Net Int.	Error %	R	A	F
C K	72.4	77.8	6148.8	9.0	0.9395	0.2011	1.0000
O K	27.5	22.2	2153.0	10.8	0.9470	0.0726	1.0000
Al K	0.1	0.1	82.9	6.8	0.9604	0.6153	1.0033

3.3.XRD analysis.

Figure 7shows the XRD patterns of the CB filler. The XRD signals of the powdered sample contain several peaks that validate carbon's amorphous behavior. It is also observed that the sharpness of the peaks increases in the filler material. The structural ordering of CB filler has been evaluated by the lattice parameters d_{002} and L_a and comparing the broadening/ sharpening of their diffraction profiles (002) and (100). It is observed that the broad profiles

are gradually sharpened, and there is a very small annular shifting of the lines in the graphite characteristic path. The carbon content rises due to the carbonization of OP particulates. Some small peaks are also observed in CB filler due to the presence of SiO_2, Al_2O_3, and MgO.

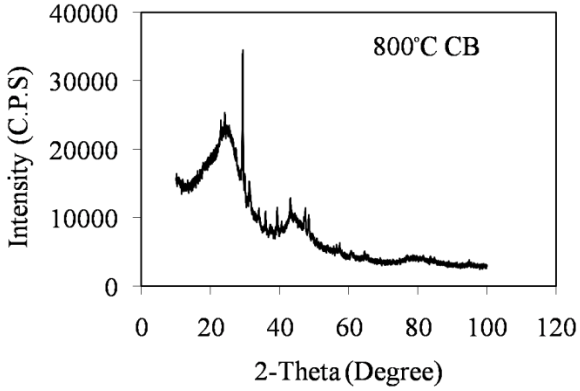

Figure 7. XRD analysis of carbon black filler.

3.4.Effect of impact angle (α) on EW of CB composites.

Figure 8showsthe effect of impact angle on the erosion rate of CB-reinforced composite material at different erodent velocities. It is found that erosion resistance was significantly developed due to the incorporation of CB fillers into the epoxy matrix. The maximum EW is observed at 45° impact angle for all filler loadings at low velocity, i.e., 48 m/s; therefore, the developed composite is semi-ductile in nature. However, maximum erosion was recorded at a 60° impact angle for high velocities, such as 70 m/s and 82 m/s. So the specimen behaves semi-brittle nature at a higher impact velocity. The material removed from the specimen is mainly due to the shearing action of erodent particles at low velocity. In contrast, at a higher velocity, the impact of erodent plays a vital role in removing the material. Impact velocity has a very strong influence on wear rate. Similar behavior was also observed by Pradhan and Acharya [8] while studying the solid particle EW behavior of *Eulaliopsis binata* fiber-reinforced epoxy composites. The EW rate is the minimum for the CB filler composite at all impact velocities. This is attributed to the presence of porous structures and high carbon content in filler material confirmed from the SEM and EDX analysis, respectively. The increase in wear resistance of S4 composite material is due to the presence of rigid biochar and good interfacial bonding between filler and matrix material.

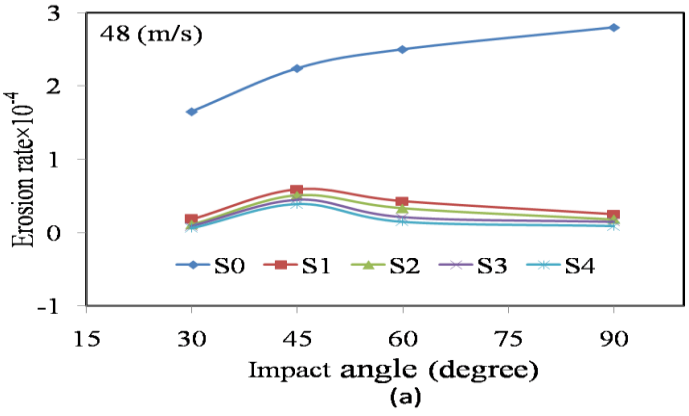

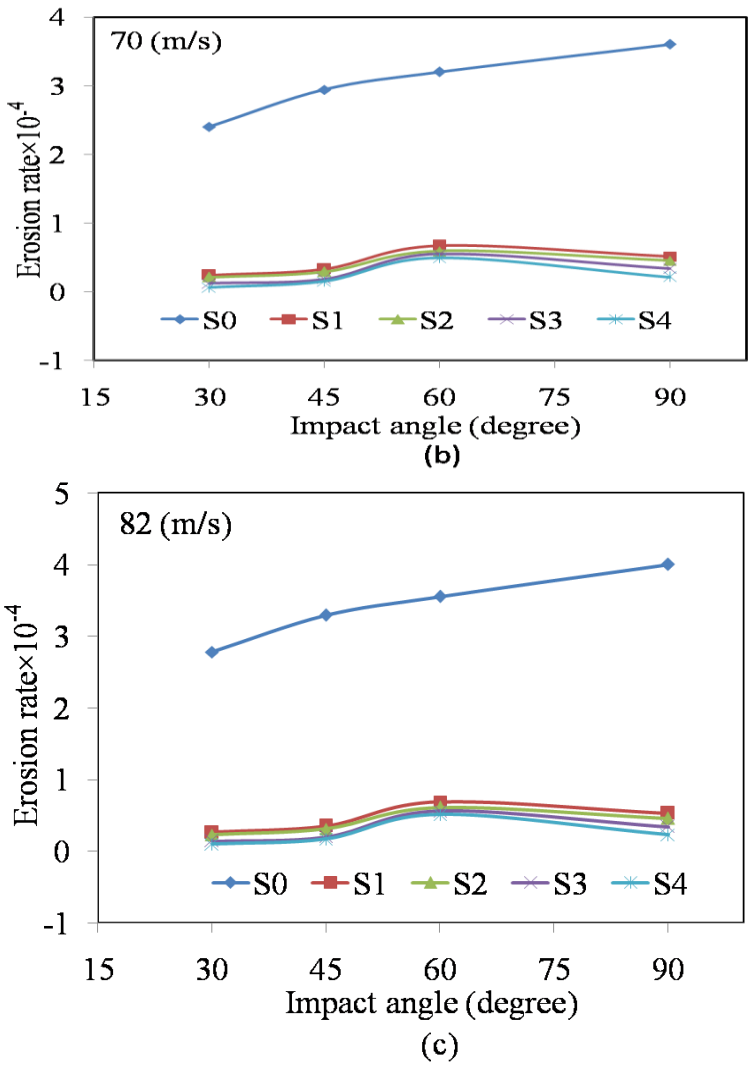

Figure 8. Erosion wear rate of S4 composites reinforced with CB filler materials at **(a)** 48 m/s, **(b)** 70 m/s, and **(c)** 82 m/s. [Note: S0, S1, S2, S3, and S4 represent pure epoxy, 5, 10, 15, and 20 wt% of CB composites, respectively].

3.5.Effect of filler loadings on EW of CB composites

Figure 9 shows the variation of EW of different specimens with respect to different filler loadings at different impact angles and impact velocities. The figure shows that the EW resistance increases with an increase in filler loadings irrespective of impact velocities and angle. The S4 specimen has the lowest EW rate in comparison to other filler loadings. The high wear resistance may be due to the CB filler's microporous structure and hard carbon elements. Due to carbonization, the adsorption capacity and surface area of the filler materials increase. The particle size is reduced by increasing the surface area. So, the distribution of the carbonization particles in epoxy is increased. Hence, there is strong interfacial bonding between CB filler and epoxy matrix. This is the reason for the increase inerosion resistance, and the maximum is observed in the case of 20 wt% filler loadings. Khalil *et al*. [31]Also, there is a strong interfacial bonding between epoxy and CB filler. They extracted CB filler from coconut shells, bamboo stems, and oil palm empty fiber branches.

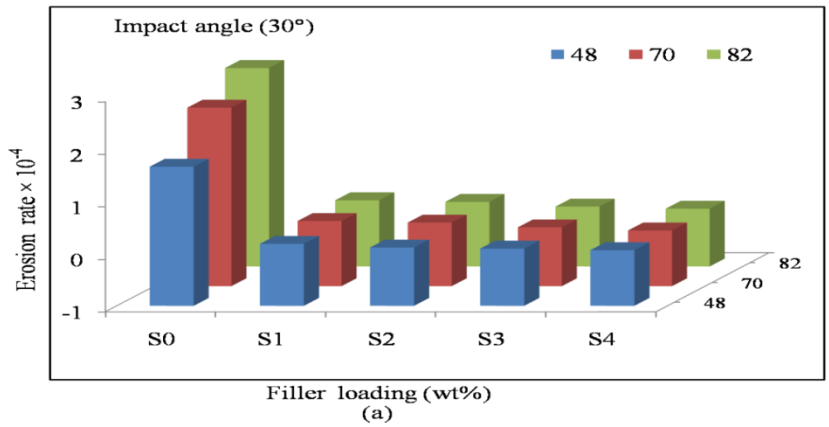

(a)

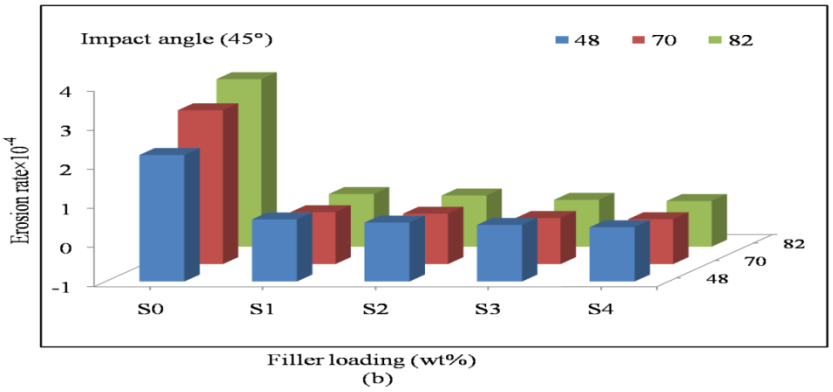

(b)

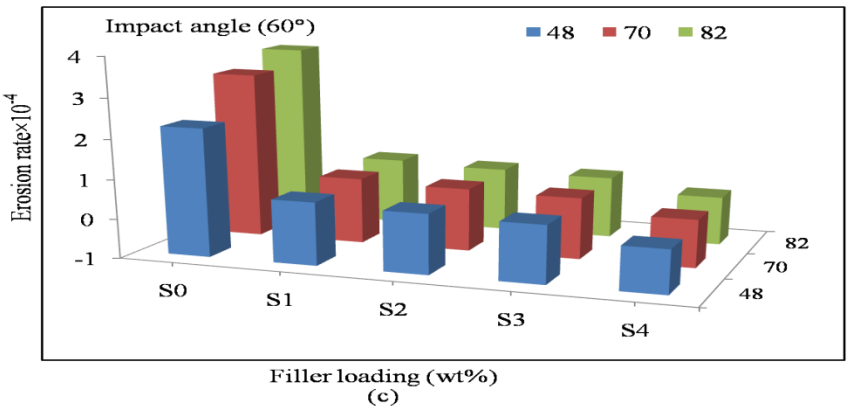

(c)

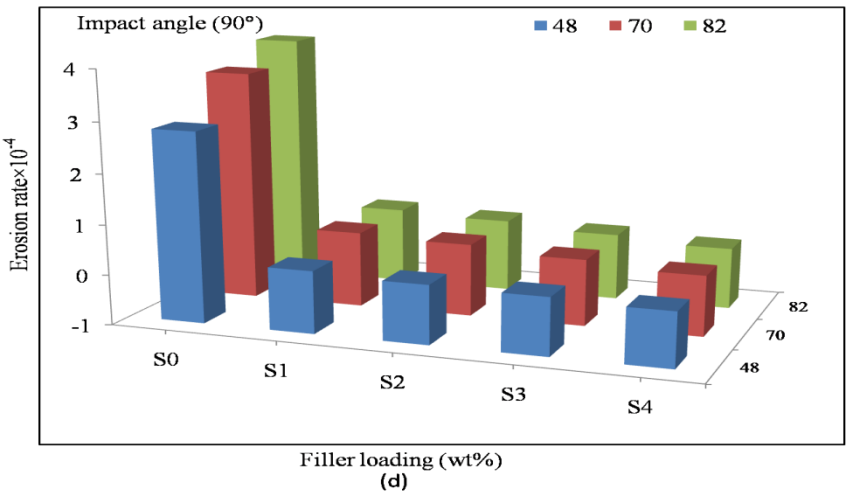

(d)

Figure 9. EW rate at 600ºC temperature: **(a)** 30º, **(b)** 45º, and **(c)** 60º.

3.6.Effect of Impact velocity (υ) on erosion rate of CB composite.

From the experimental results, it is noticed that the erodent velocity (υ) has a strong influence on erosion behavior. The higher the impact velocity, more is the EW rate of fabricated composite materials. At higher velocities, the K.E. of the erodent particle is transformed to a targeted area that deforms the material plastically and separates the fillers from the matrix. Therefore, the damage in the specimen at high impact velocities is due to the formation of craters and micro-cuts which are developed due to the repeated strikes of hard erodent particles. This is attributed to increases in the wear rate at higher impact velocities. Figure 10 shows the variation of EW w. r. t the impact velocity at different impact angles for CB composites. At a low impact velocity, the variation of EW is very less compared to the higher impact velocity.

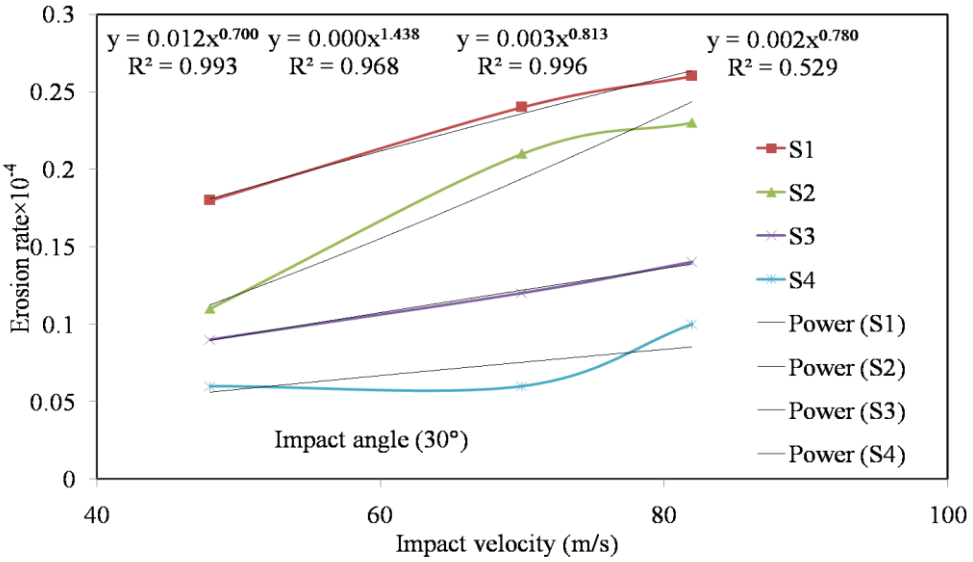

(a)

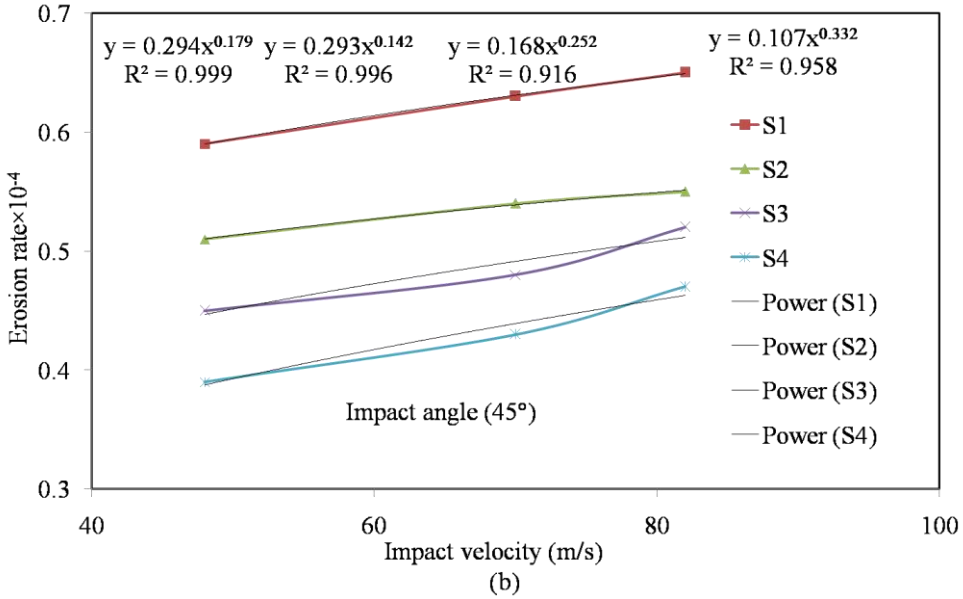

(b)

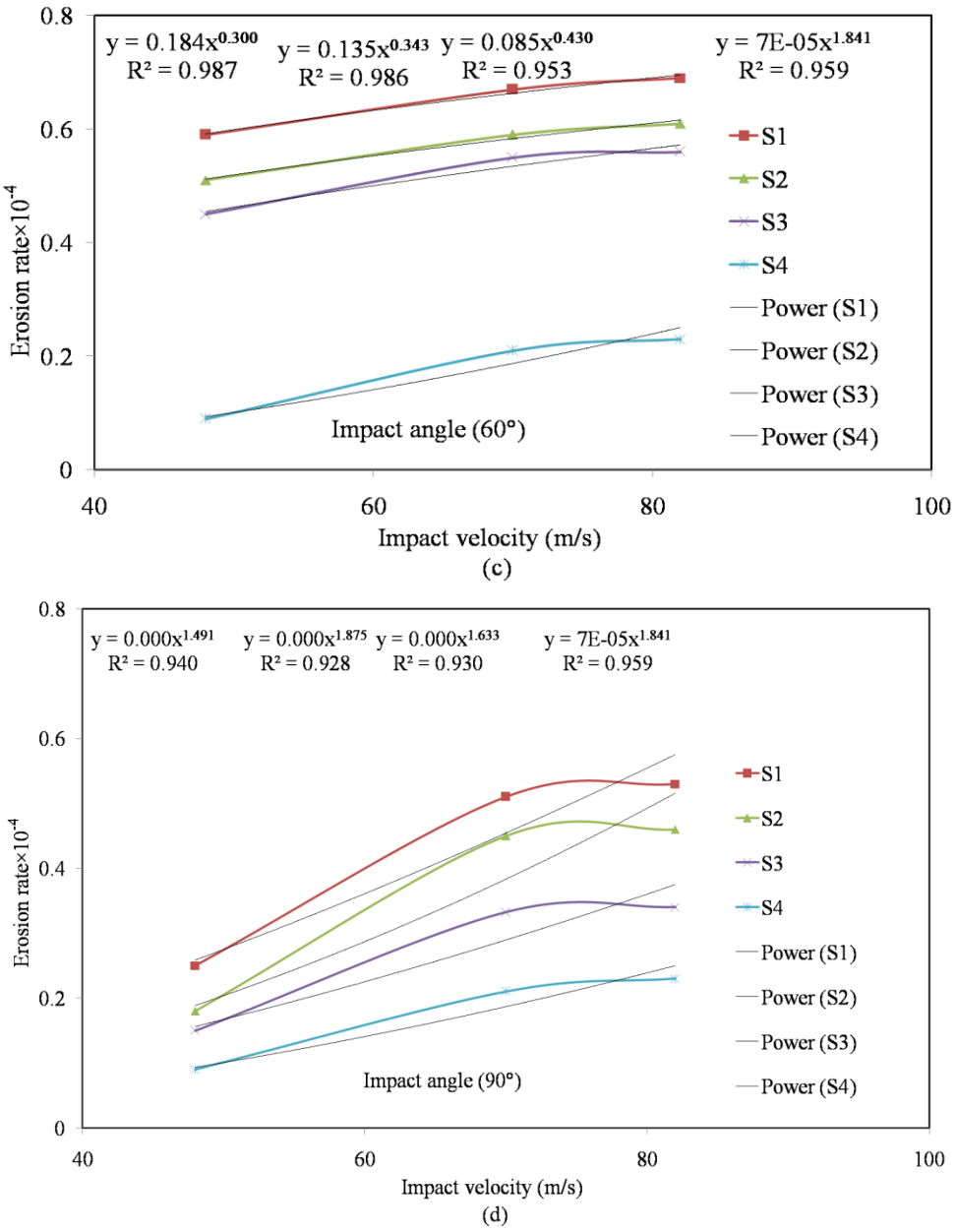

Figure 10. Variation of EW rate at 600°C at different angles: **(a)** 30°, **(b)** 45°, **(c)** 60°, and **(d)** 90°.

At low velocity, the stress developed at the impact point is not enough to produce plastic deformation and wear fatigue. Therefore, the EW rate increases gradually as the velocity increases from 48 m/s to 82 m/s, as shown in Figure 10.

Once the steady state condition is reached, the erosive wear (E_r) can be calculated using the equation. From Figure 10, the velocity exponents recorded for different impingement angles are in the range of 2.33–2.96, 1.35–1.8, 2.06–2.68, and 2.34-2.58, respectively, for the CB composites with maximum value at a 60° impact angle. The velocity exponents (n) were in the range of 1.35 to 2.965 for the CB-reinforced composite materials at different impingement angles. Therefore, the CB-reinforced epoxy composites exhibit semi-ductile behavior, and the velocity exponents conform with Pool *et al*. [32].

3.7.Erosion efficiency.

The erosion efficiency (η) is another important parameter in studying polymeric material's brittle and ductile response. It can be calculated by using the equation $\eta =$

$2E_rH/2\rho v^2$. H is the hardness, ρ is the density of the target material, and v is the impact velocity. η of polymeric material may be zero, one, or sometimes greater than unity as per the behavior of the polymeric composite material towards EW. When $\eta=0$, there is almost no erosion, and a very small amount of material is removed from the surface of the targeted material without developing any fracture. When $0<\eta<1$, erosion happens due to crater formation, and fracture occurs.

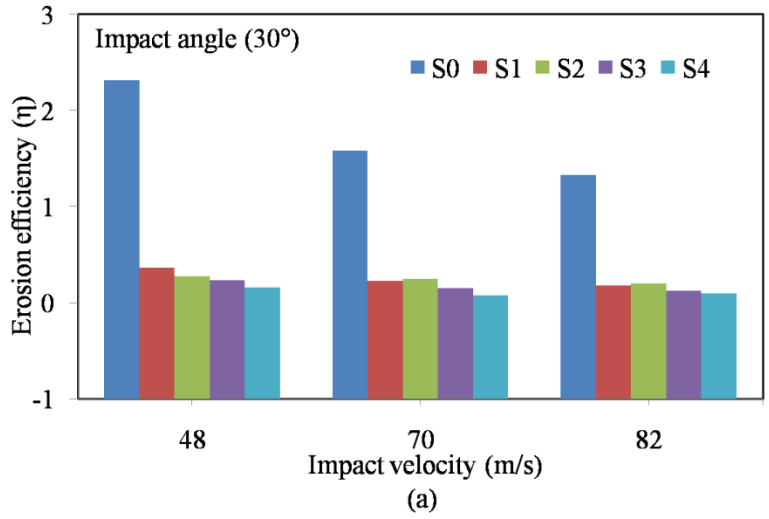

(a)

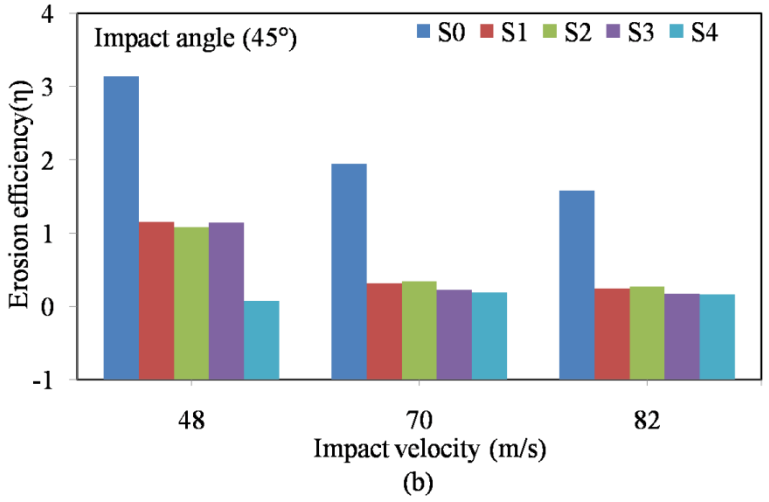

(b)

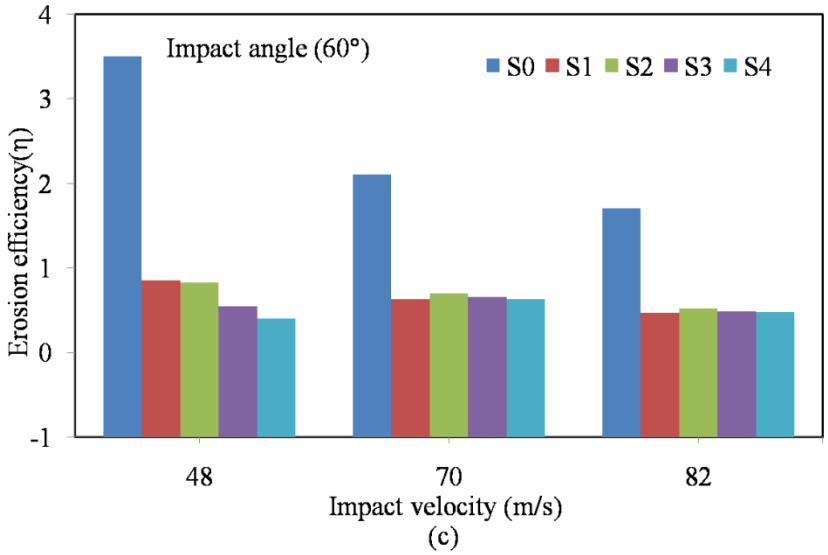

(c)

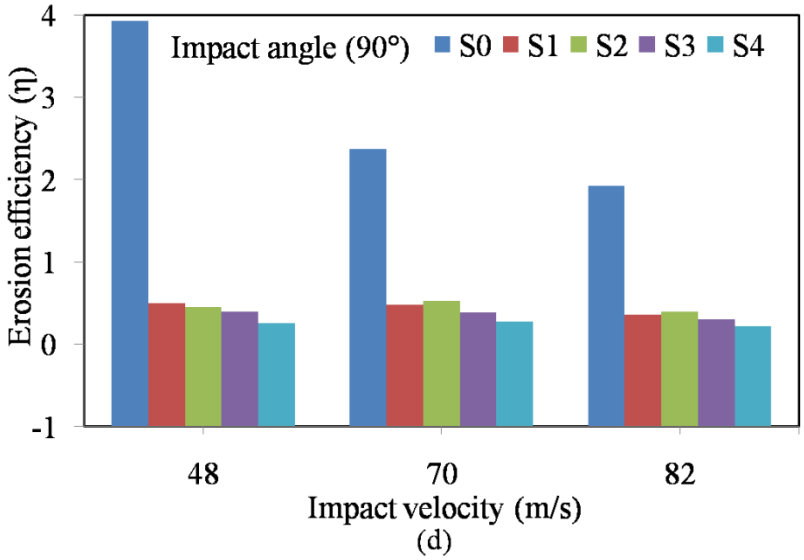

Figure 11. Erosion efficiency as a function of impact velocity for CB reinforced epoxy composites.

The erosion occurs due to material spalling and removal of large chunks in the case of brittle material where η>1. The lower erosion efficiency of 20 wt% CB filler composite indicates better erosive resistance. Since the CB-reinforced composite material's EW increases with impact velocity, η also increases with the increase in velocity. From Figure 11, it has been observed that the η value varies from 0.9 to 4.1 at different impact velocities that have been studied. Thus, it is concluded that the EW of CB-reinforced composite material is due to micro-plowing, micro-cutting, and micro-cracking. From the above discussions, it is concluded that the developed specimen is semi-ductile in nature. The value of η of S4 composite has the lowest among all fabricated composites irrespective of impact angle and impact velocity.

3.8. Surface examination.

The K.E. of the erodent particles used for the EW analysis is responsible for plastic deformation, such as the development of micro cracks, crater formation, and debonding of filler matrix material in the targeted composite material [33]. The morphology of erodent particle surfaces is presented in Figure 12.

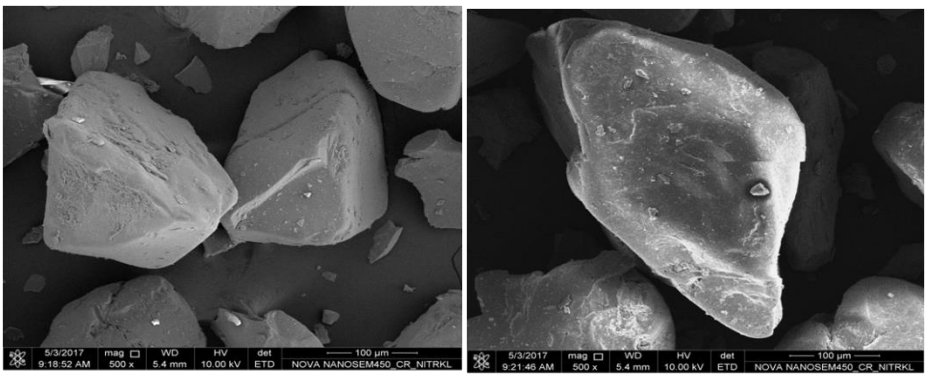

Figure 12. SEM. of the erodent particles.

The SEM features of worn surfaces S2 composite at different erodent velocities (low (48 m/s) and high (82 m/s)) under constant working parameters is presented in Figure 13. At a lower erodent velocity, the MRR is minimal, as shown in Figure 13 (a). The micro-cuts, micro-

cracks, and small craters are distinctly visible on the eroded specimen. Similar results were also observed by Vigneshwaran *et al*. [34] while studying the solid particle erosion of sisal/polyester hybrid composites reinforced with red mud (industrial waste). It is observed that there is a detachment of filler material from the matrix at 82 m/s. This may be due to compressive stress developed on the material's surface due to the penetration of erodent particles. The cavities are formed due to the high MRR of filler material from the surface of the composites. The distorted surface and crater are clearly visible, as shown in Figure 13 (b). The morphological analysis validates the results obtained from the experiments.

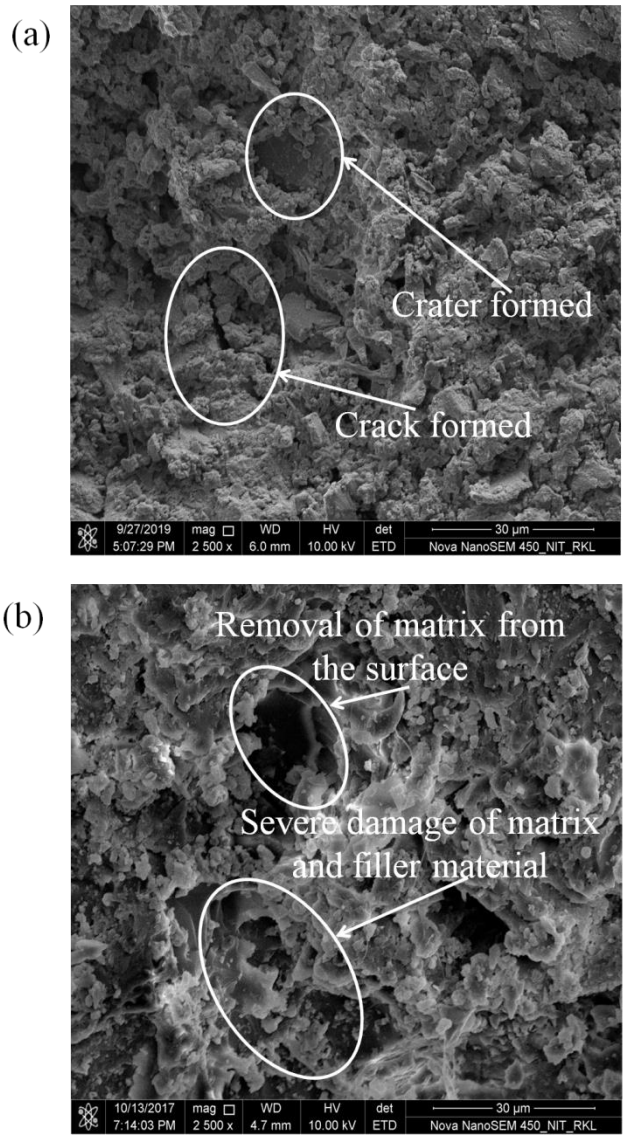

Figure 13. SEM analysis of worn S2 composite: **(a)** erodent velocity 48 m/s and **(b)** erodent velocity 82 m/s.

SEM analyses of different specimens (S1, S2, and S4) under a specified operating condition (erodent velocity 48 m/s, and impact angle 45^{o}) are shown in Fig. 14. With the increase in wt % percentage of filler, the amount of material removed from the surface decreases (as shown in Fig. 14). This is attributed to strong bonding between the components of the specimen. Due to the low wt % of filler material, weak bonds between the matrix materials are present, leading to generating the crack lines along the surface (Figure 14(a)). Also, micro-cracks are generated on the specimen's surface in the absence of filler material due to localized fragmentation of matrix material. This is attributed to the poor bond strength and agglomeration of filler material. From Figure 14(b), it is observed that the MRR is decreased

by adding the filler material by absorbing energy waves which are developed due to the striking of erodent particles on the surface of composite material. With an increase in the filler loading, the debonding between the matrix and filler material is clearly noticeable in the crater development area. This is attributed to inadequate filler material to absorb the shock due to impingement particles. Furthermore, adding filler material reduces the EW due to the uniform distribution of filler material and strong interfacial bonding between the matrix and reinforcement. The fabricated composite material foiled the indentation and absorbedthe energy developed due to impingement particles(Figure 14(c)). The SEM analysis reveals that filler loadings play an important role in the EW mechanism.

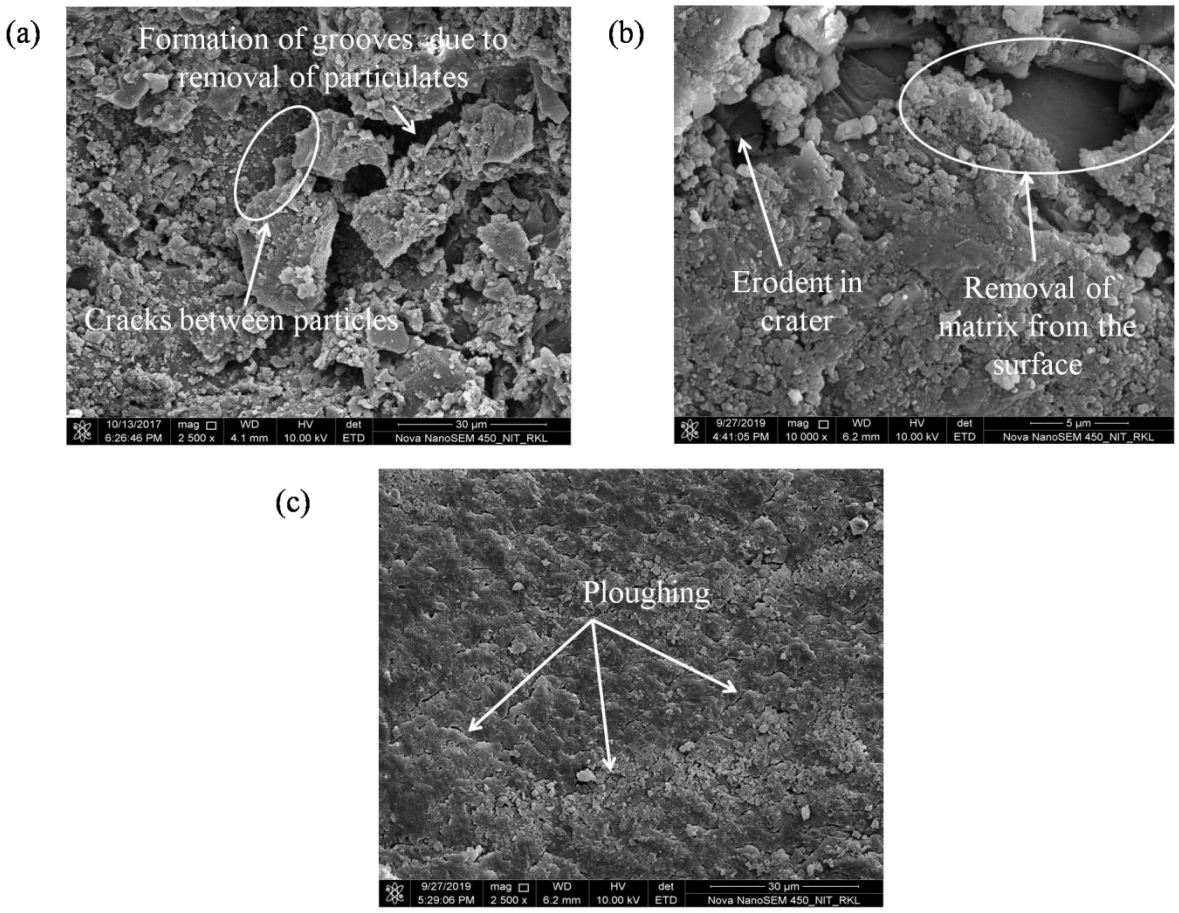

Figure 14. SEM analysis at 48 m/s (impact velocity) and impact angle 45°**(a)** S1 composite, **(b)** S2 composite, and **(c)** S4 composite.

The worn surface of the S4 composite at 60° impact angle at low velocity (82 m/s) is given in Figure 15. Craters are observed on the sample's surface in Figure 15 (a). The erodent particle velocity can produce cracks/plowing/micro grooves on the surface of the specimen due to force in the normal direction. Due to higher impact velocity, the filler material was pulled out from the surface of the specimen, and the material removal rate increased. However, in Figure 15(b), there is no sign of detachment of filler material. Cracks are formed due to high impact velocity.

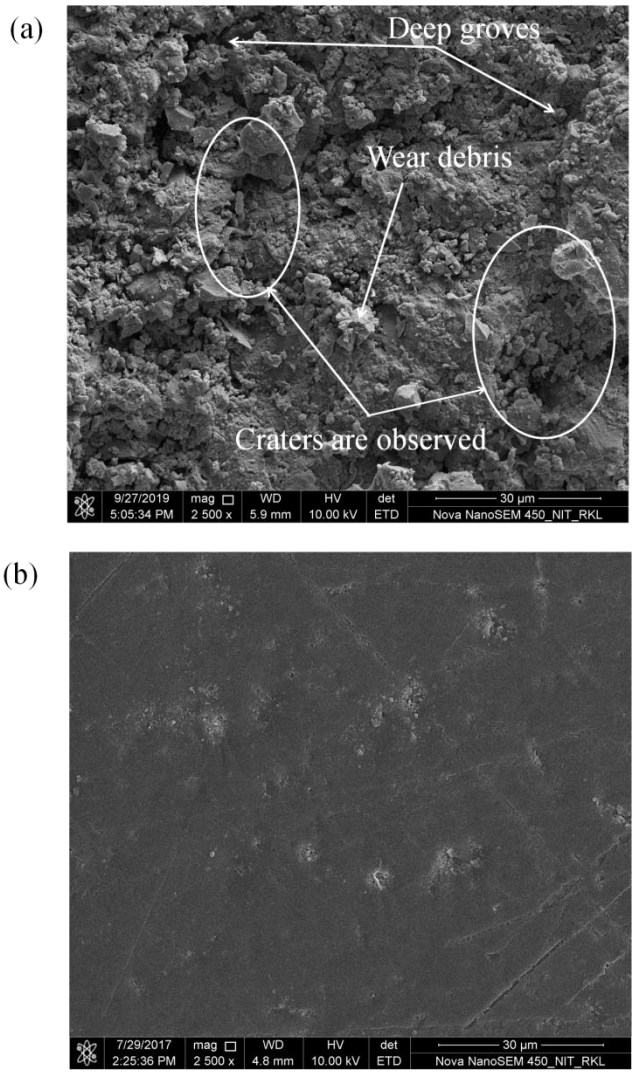

Figure 15. SEM analysis of worn S4 composite with impact angle **(a)** at 60º and **(b)** at 45º under 80 m/s.

The worn surfaces of S1 and S4 composite specimens under a specified operating condition, i.e., 48 m/s and at 30º impact angle, are shown in Figure 16. Due to strong interfacial adhesion between filler and matrix, less number of grooves are formed, and minor cracks are visible after the continuous bombardment of erodent on the targeted surface. As a result, voids and filler chips are not seen on the surface of the composite material.

The SEM analysis reveals that solid particle erosion happens due to several stages of material removal processes. At the beginning of the experiment, the matrix material was separated from the composite due to the bombardment of sand particles; as a result, the reinforcement material was exposed. Subsequently, crack formation and breakage occurred after the repeated striking of the hard silica particles on the target surface, which is observed from SEM analysis.

The present study considers carbon black obtained from orange peel to use as a filler in the composite and evaluates its erosion wear behavior. To improve the durability of the composite, one can adopt different surface coatings, including electroless nickel [35-40], where a thin nickel-based coating helps improve protection against surface damage. Accordingly, this can be an area for future study apart from evaluating orange peel-based epoxy composites [41-42].

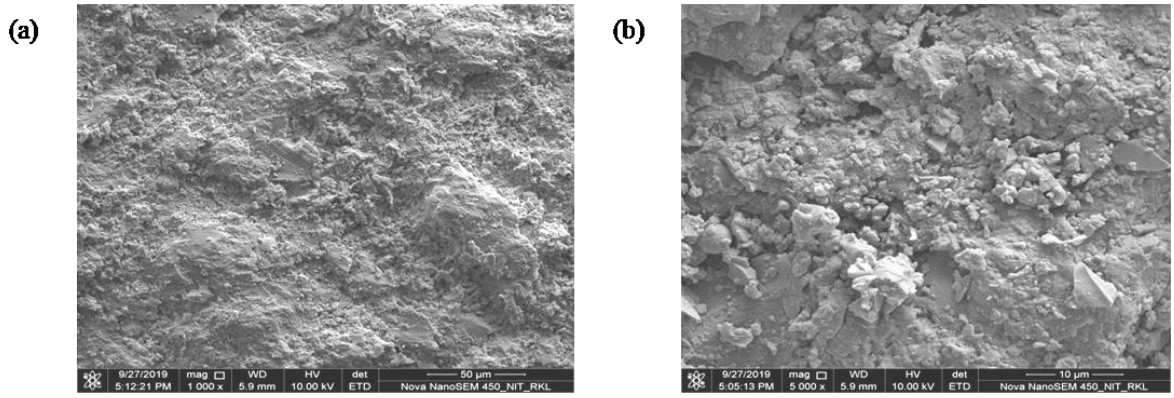

Figure 16. SEM image of worn surfaces: **(a)** S1 and **(b)** S4 composites.

4. Conclusions

In the present work, the specimens were fabricated by traditional hand lay-up technique with varying wt fractions of CB (5%, 10%, 15%, and 20%) filler material. The erosion rate of fabricated specimens was examined under different operating conditions, such as impact angle and impact velocity. CB filler was synthesized by pyrolysis method from OPP at 800°C temperature. CB, as a filler in the composite industry, is expected to get low-cost, environmentally friendly, and enhanced-performance materials. The subsequent findings drawn from the present work are given below: The experimental results illustrate that the brittle behavior of pure epoxy changes to ductile behavior during erosive wear analysis due to the addition of CB filler; The operating parameters used to analyze fabricated specimens indicate a significant effect on EW behavior.The minimum EW rate is recorded in the case of 20 wt % CB specimen, i.e., erosion strength is higher than other fabricated composite material; It is confirmed that the impact velocity is the major factor that influences the EW of fabricated composite materials irrespective of the filler loadings, i.e., the erosion rate increases with increasing the erodent velocity. It is found that the erosive wear behavior followed the power law with respect to impact velocities. It is confirmed that the fabricated materials show semi-ductile behavior towards EW; The worn surfaces of testing samples were examined by SEM analysis which confirmed that the overall damage in the fabricated specimen is due to weak interfacial bonding between epoxy and CB filler. So there is a high MRR at low filler loadings. The EW mechanism and MRR were also revealed by SEM analysis.

Funding

This research received no external funding.

Acknowledgments

None.

Conflicts of Interest

The authors declare no conflict of interest.

References

1. Wang, H.; Menon, H.; Hassan, M.; Miah, E.; Ali, M. Effect of jute fiber modification on mechanical properties of jute fiber composite. *Materials* **2019**, *12*, 1226, https://doi.org/10.3390/ma12081226.

2. Adeniyi, A.G.; Onifade, D.V.; Ighalo, J.O.; Adeoye, A.S.. A review of coir fiber reinforced polymer composites. *Composites Part B: Engineering* **2019**, *176*, p.107305, https://doi.org/10.1016/j.compositesb.2019.107305. .
3. Alemayehu, Z.; Nallamothu, R.B.; Liben, M.; Nallamothu, S.K.; Nallamothu, A.K. Experimental investigation on characteristics of sisal fiber as composite material for light vehicle body applications. *Materials Today: Proceedings* **2021**, *38*, 2439-2444, https://doi.org/10.1016/j.matpr.2020.07.386.
4. Mishra, V.; Agrawal, A. Eco-Friendly Epoxy-Based Composites. *Epoxy Composites: Fabrication, Characterization and Applications* **2021**, 97-123, Wiley,https://doi.org/10.1002/9783527824083.ch5.
5. Abdelbary, A.; Mohamed, Y.S. Tribological behavior of fiber-reinforced polymer composites. *Tribology of Polymer Composites* **2021**, 63-94, Elsevier, https://doi.org/10.1016/B978-0-12-819767-7.00004-9.
6. Naik, P.; Acharya, S.K.; Sahoo, P.; Pradhan, S. Abrasive wear behavior of orange peel (biowaste) particulate reinforced polymer composites. *Proceedings of the Institution of Mechanical Engineers, Part J: Journal of Engineering Tribology* **2021**, *235*, 2099-2109, https://doi.org/10.1177/1350650121991412.
7. Sydow, Z.; Sydow, M.; Wojciechowski, Ł.; Bieńczak, K. Tribological performance of composites reinforced with the agricultural, industrial and post-consumer wastes: A review. *Materials* **2021**, *14*, 1863, https://doi.org/10.3390/ma14081863.
8. Pradhan, S.; Acharya, S.K. Solid particle erosive wear behavior of *Eulaliopsis binata* fiber reinforced epoxy composite. *Proceedings of the Institution of Mechanical Engineers, Part J: Journal of Engineering Tribology* **2021**, *235*, 830-841, https://doi.org/10.1177/1350650120931645.
9. Pujari, S.; Srikiran, S. Experimental investigations on wear properties of Palm kernel reinforced composites for brake pad applications. *Defence Technology* **2019**, *15*, 295-299, https://doi.org/10.1016/j.dt.2018.11.006.
10. Harsha, A.P.; Thakre, A.A., Investigation on solid particle erosion behavior of polyetherimide and its composites. *Wear* **2007**, *262*, 807-818, https://doi.org/10.1016/j.wear.2006.08.012.
11. Roy, M.; Vishwanathan, B.; Sundararajan, G. The solid particle erosion of polymer matrix composites. *Wear* **1994**, *171*, 149-161, https://doi.org/10.1016/0043-1648(94)90358-1.
12. Srivastava, V.K.; Pawar, A.G.. Solid particle erosion of glass fibre reinforced flyash filled epoxy resin composites. *Composites Science and Technology* **2006**, *66*, 3021-3028, https://doi.org/10.1016/j.compscitech.2006.02.004.
13. Gupta, A. Influence of Filler Content on Tribological Behavior of Cenopshere Flyash Filled Bamboo Fiber Reinforced Composites. *Journal of Natural Fibers* **2022**, pp.1-17, https://doi.org/10.1080/15440478.2022.2051666.
14. Naik, P.; Sahoo, P.; Acharya, S. K.; Pradhan, S. Erosive wear behavior of bio-waste particulate-reinforced epoxy composites for low cost applications. *Journal of the Indian Academy of Wood Science* **2021**, *18*, 1-13, https://doi.org/10.1007/s13196-020-00272-y.
15. Nayak, S.; Mohanty, J. Erosion wear behavior of benzoyl chloride modified areca sheath fiber reinforced polymer composites. *Composites Communications* **2020**, *18*, 19-25, https://doi.org/10.1016/j.coco.2020.01.006.
16. Antil, P.; Singh, S.; Kumar, S.; Manna, A.; Pruncu, C.I. Erosion analysis of fiber reinforced epoxy composites.*Materials Research Express***2019**, *6*, 106520, https://doi.org/10.1088/2053-1591/ab34b4.
17. Imoisili, P.E.; Jen, T.C. Mechanical and water absorption behavior of potassium permanganate (KMnO4) treated plantain (Musa Paradisiacal) fibre/epoxy bio-composites. *Journal of Materials Research and Technology* **2020**, *9*, 8705-8713, https://doi.org/10.1016/j.jmrt.2020.05.121.
18. Naik P.; Pradhan S.; Sahoo P.; Acharya S K. Effect of filler loading on mechanical properties of natural carbon black reinforced polymer composites. *Materials Today: Proceedings* **2020**; *26*, 1892-1896, https://doi.org/10.1016/j.matpr.2020.02.414.
19. Minugu, O.P.; Panchal, M.; Gujjala, R.; Ojha, S.; Krzyzak, A.; Kumar, D. Effect of biomass-biochar content on the erosion wear performance of biochar epoxy composites. *Polymer Composites* **2022**, *43*, 3189-3203, https://doi.org/10.1002/pc.26610.
20. Johnson, R. D. J.; Arumugaprabu, V.; Kumar, M. P.; Dheeraj, K. Solid particle erosion on the biochar filled hybrid vinyl ester composite.*AIP Conference Proceedings* **2019**, *2057*, 020064, https://doi.org/10.1063/1.5085635.
21. Sutikno, M.; Marwoto, P.; Rustad, S. The mechanical properties of carbonized coconut char powder-based friction materials. *Carbon* **2010**, *48*, 3616-3620, https://doi.org/10.1016/j.carbon.2010.06.015.

22. Shakuntala, O.; Raghavendra, G.; Samir Kumar, A. Effect of filler loading on mechanical and tribological properties of wood apple shell reinforced epoxy composite.*Advances in Materials Science and Engineering* **2014**, https://doi.org/10.1155/2014/538651.
23. Samantrai, S.P.; Raghavendra, G.; Acharya, S.K. Effect of carbonization temperature and fibre content on the abrasive wear of rice husk char reinforced epoxy composite. *Proceedings of the Institution of Mechanical Engineers, Part J: Journal of Engineering Tribology* **2014**, *228*, 463-469, https://doi.org/10.1177/1350650113516435.
24. Betancourt, S.; Cruz, L.J.; Toro, A. Effect of the addition of carbonaceous fibers on the tribological behavior of a phenolic resin sliding against cast iron. *Wear* **2011**, *272*, 43-49, https://doi.org/10.1016/j.wear.2011.07.014.
25. Giorcelli, M.; Khan, A.; Pugno, N.M.; Rosso, C.; Tagliaferro, A. Biochar as a cheap and environmental friendly filler able to improve polymer mechanical properties. *Biomass and bioenergy* **2019**, *120*, 219-223, https://doi.org/10.1016/j.biombioe.2018.11.036.
26. Bath, F. Consistent milling on a nano scale. *Ceramic Industry* **2005**, *155*, 26-28, https://www.researchgate.net/publication/294408889_Consistent_milling_on_a_nano_scale.
27. Sundararajan, G.; Roy, M.; Venkataraman, B. Erosion efficiency-a new parameter to characterize the dominant erosion micromechanism. *Wear* **1990**, *140*, 369-381, https://doi.org/10.1016/0043-1648(90)90096-S.
28. Tilly,G.P. A two stage mechanism of ductile erosion. *Wear* **1973**, *23*, 87-96, https://doi.org/10.1016/0043-1648(73)90044-6.
29. Prakash, M.O.; Raghavendra, G.; Ojha, S.; Panchal, M.; Kumar, D. Investigation of tribological properties of biomass developed porous nano activated carbon composites. *Wear* **2021**, *466*, 203523, https://doi.org/10.1016/j.wear.2020.203523.
30. Arjula, S.; Harsha, A.P.; Ghosh, M.K. Solid-particle erosion behavior of high-performance thermoplastic polymers. *Journal of Materials Science* **2008**, *43*, 1757-1768, https://doi.org/10.1007/s10853-007-2405-0.
31. Khalil, H.A.; Firoozian, P.; Bakare, I.O.; Akil, H.M.; Noor, A.M. Exploring biomass based carbon black as filler in epoxy composites: Flexural and thermal properties. *Materials & Design* **2010,** *31*, 3419-3425, https://doi.org/10.1016/j.matdes.2010.01.044.
32. Pool, K.V.; Dharan, C.K.H.; Finnie, I. Erosive wear of composite materials. *Wear* **1986**, *107*, 1-12, https://doi.org/10.1016/0043-1648(86)90043-8.
33. Biswas, S.; Satapathy, A. Tribo-performance analysis of red mud filled glass-epoxy composites using Taguchi experimental design. *Materials & Design* **2009**, *30*, 2841-2853, https://doi.org/10.1016/j.matdes.2009.01.018.
34. Vigneshwaran, S.; Uthayakumar, M.; Arumugaprabu, V. Solid particle erosion study on redmud-an industrial waste reinforced sisal/polyester hybrid composite. *Materials Research Express* **2019**, *6*, 065307, https://doi.org/10.1088/2053-1591/ab0a44.
35. Banerjee, S.; Sarkar, P.; Sahoo, P. Improving corrosion resistance of magnesium nanocomposites by using electroless nickel coatings. *Facta Universitatis, Series: Mech Engg* **2021**, 1-18, http://casopisi.junis.ni.ac.rs/index.php/FUMechEng/article/view/7833.
36. Mukhopadhyay, A.; Sahoo, S. A Grey-Fuzzy based approach for the optimization of corrosion resistance of rebars coated with ternary electroless nickel coatings. *Journal of Soft Computing in Civil Engineering* **2022**, *6*, 107-127, https://dx.doi.org/10.22115/scce.2022.326903.1401.
37. Mukhopadhyay, A.; Sahoo, S. Optimized electroless Ni-Cu-P coatings for corrosion protection of steel rebars from pitting attack of chlorides. *Engineering Transactions* **2021**, *69*, 315-332, https://entra.put.poznan.pl/index.php/et/article/viewFile/1367/903.
38. Mukhopadhyay, A.; Sahoo, S. Improving corrosion resistance of reinforcement steel rebars exposed to sulphate attack by the use of electroless nickel coatings. *European Journal of Environmental and Civil Engineering* **2021**, 1-16, https://www.tandfonline.com/doi/abs/10.1080/19648189.2021.1886177.
39. Mukhopadhyay, A.; Sahoo, S. Corrosion Performance of Steel Rebars by Application of Electroless Ni-P-W Coating-An Optimization Approach using Grey Relational Analysis, *FME Transactions* **2021**, *49*, 445-455, https://scindeks.ceon.rs/article.aspx?artid=1451-20922102445M.
40. Biswas, P.; Das, S. K.; Sahoo, P. Duplex electroless Ni-P/Ni-P-W coatings: Effect of heat treatment on tribological and corrosion performance, *Materials Today: Proceedings* **2022**, https://doi.org/10.1016/j.matpr.2022.06.042.

41. Naik, P.; Pradhan, S.; Acharya, S. K.; Sahoo, P. Effect of Pretreatment on the Mechanical Properties of Orange Peel Particulate (Bio-Waste)-Reinforced Epoxy Composites. *International Journal of Manufacturing, Materials, and Mechanical Engineering* **2022**, *12*, 1-25, http://doi.org/10.4018/IJMMME.293223.
42. Naik, P.; Pradhan, S.; Acharya, S. K.; Sahoo, P. Effect of Carbonization of Orange Peel Particulate-Reinforced Polymer Composites: Mechanical and Morphological Properties. *International Journal of Surface Engineering and Interdisciplinary Materials Science* **2022**, *10*, 1-20, http://doi.org/10.4018/IJSEIMS.295097.